ornl

OAK RIDGE
NATIONAL
LABORATORY

PHYSICS
DIVISION
PREPRINT

# FLUCTUATIONS IN TRANSVERSE ENERGY AND MULTIPLICITY, ENERGY DENSITIES, AND NEUTRAL PION SPECTRA IN NUCLEUS-NUCLEUS COLLISIONS AT 200 GeV/NUCLEON


**WA80 Collaboration**

F. Plasil, R. Albrecht, T. C. Awes, C. Baktash, P. Beckmann, F. Berger, R. Bock, G. Claesson, G. Clewing, L. Dragon, A. Eklund, R. L. Ferguson, A. Franz, S. Garpman, R. Glasow, H. A. Gustafsson, H. H. Gutbrod, J. Idh, P. Jacobs, K. H. Kampert, B. W. Kolb, P. Kristiansson, I. Y. Lee, H. Löhner, I. Lund, F. E. Obenshain, A. Oskarsson, I. Otterlund, T. Peitzmann, S. Persson, A. M. Poskanzer, M. Purschke, H. G. Ritter, S. Saini, R. Santo, H. R. Schmidt, T. Siemiarczuk, S. P. Sorensen, K. Steffens, E. Stenlund, D. Stüken, M. L. Tincknell, G. R. Young



*– Invited Paper –*

*International Workshop on Relativistic Aspects of Nuclear Physics, Rio de Janeiro, Brazil, August 28–31, 1989*


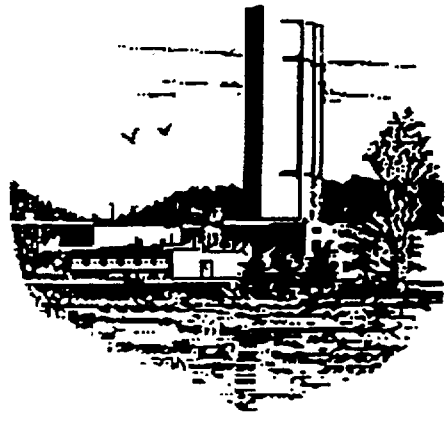

## DISCLAIMER

CONF-890826--3

DE89 017583

# FLUCTUATIONS IN TRANSVERSE ENERGY AND MULTIPLICITY, ENERGY DENSITIES, AND NEUTRAL PION SPECTRA IN NUCLEUS-NUCLEUS COLLISIONS AT 200 GeV/NUCLEON

**WA80 Collaboration**

F. Plasil,[a] R. Albrecht,[b] T. C. Awes,[a] C. Baktash,[a] P. Beckmann,[c] F. Berger,[c] R. Bock,[b] G. Claesson,[b] G. Clewing,[c] L. Dragon,[c] A. Eklund,[d] R. L. Ferguson,[a] A. Franz,[e,f] S. Garpman,[d] R. Glasow,[c] H. A. Gustafsson,[d] H. H. Gutbrod,[b] J. Idh,[d] P. Jacobs,[e] K. H. Kampert,[c] B. W. Kolb,[b] P. Kristiansson,[e] I. Y. Lee,[a] H. Löhner,[c] I. Lund,[b] F. E. Obenshain,[a,f] A. Oskarsson,[d] I. Otterlund,[d] T. Peitzmann,[c] S. Persson,[d] A. M. Poskanzer,[e] M. Purschke,[c] H. G. Ritter,[e] S. Saini,[a] R. Santo,[c] H. R. Schmidt,[b] T. Siemiarczuk,[b,*] S. P. Sorensen,[a,f] K. Steffens,[c] E. Stenlund,[d] D. Stüken,[c] M. L. Tincknell,[a] and G. R. Young[a]

## 1. INTRODUCTION

The main goal of the CERN heavy-ion experiments is the search for an indication that the predicted state of deconfined quarks and gluons, the quark-gluon plasma (QGP), has been produced. The quantity most crucial to the probability of QGP formation is the thermalized energy density attained during the heavy-ion reaction. The amount of energy radiated transverse to the beam direction is the experimental quantity which is believed to be a measure of the amount of energy deposition in the reaction, and hence to reflect the energy density attained. In this presentation we consider the systematics of transverse energy production at CERN SPS energies,[1-3] and we use the results to make estimates, under various assumptions, of attained energy densities.[2-5]

When extreme phenomena such as the creation of the QGP are considered, it is very important to understand the nature of events in the tails of event-characterizing distributions such as transverse energy, $E_T$, distributions. It is possible that the plasma may be created only in those events that exhibit the highest values of $E_T$ and/or particle multiplicity. We show here results of comparisons between experiment and theory of global and local fluctuations in the distributions of transverse energy and of charged particle multiplcity.[6] Starting with the observation that, in central collisions, $E_T$ and charged-particle multiplicity ($n_{ch}$) distributions

have Gaussian shapes,[7-9] we study second moments of the distributions and show how different contributions add to give the total observed widths.

Measurements of direct photons and lepton pairs are considered to be among the most promising methods for studies of the QGP. In contrast to hadrons, direct photons are not expected to undergo any interactions after their creation. The WA80 collaboration has undertaken the measurement of direct photons,[10,11] which is a difficult task due to the presence of a high background of photons from the decay of neutral pions. The $\pi^0$ spectra themselves, however, provide us with the opportunity to study the excited reaction zone during the hadronization phase. We present here measurements of neutral pions produced in $^{16}O$ + Au collisions at 200 GeV/nucleon.

## 2. EXPERIMENTAL ARRANGEMENT

A simplified version of the WA80 experimental arrangement is shown in Fig. 1. For the purpose of clarity most of the detectors used to measure the multiplicities of charged particles are not shown. The transverse energy distributions

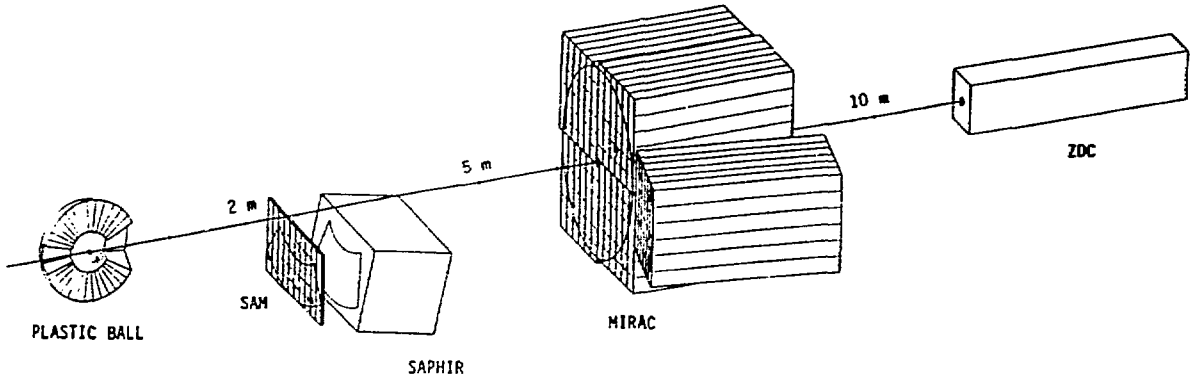


**Fig. 1.** Simplified version of the WA80 experimental setup. The target is located at the center of the Plastic Ball. SAPHIR is the single-arm photon detector. SAM is an associated charged-particle detector. MIRAC is the Midrapidity Calorimeter, and ZDC is the Zero-Degree Calorimeter. Most of the arrays used to measure the multiplicities of charged particles are not shown.

presented here were obtained with the midrapidity calorimeter MIRAC. It covers a pseudorapidity, $\eta$, interval from 2.4 to 5.5 and has full azimuthal coverage in this

$\eta$ range. The spectra of neutral pions were deduced by reconstruction from photon measurements performed with the single-arm photon spectrometer, SAPHIR.

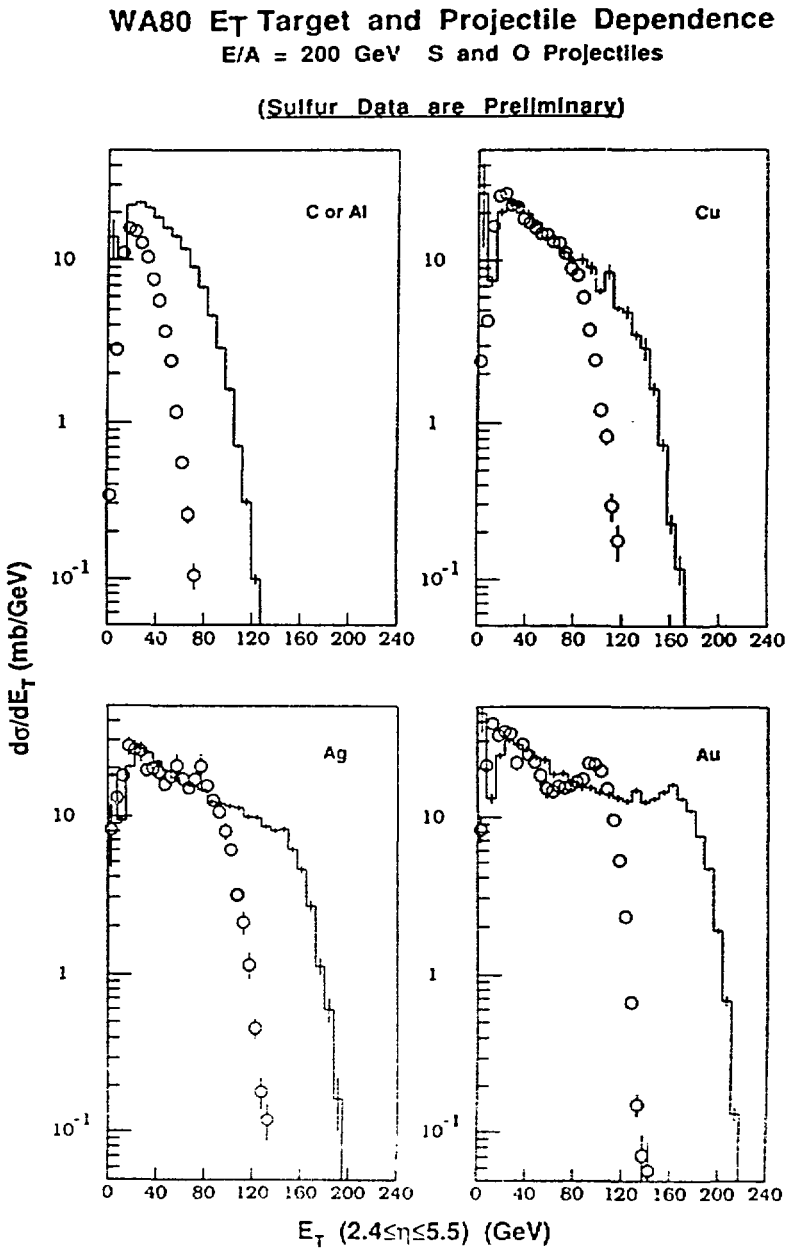


Fig. 2. Transverse energy distributions from 200-GeV/nucleon $^{16}O$ (circles) and $^{32}S$ (histograms) reactions with various target nuclei in the pseudorapidity range $2.4 \cdot \eta \cdot 5.5$. The sulfur data are preliminary.

This detector covers about one-sixth of the solid angle in the range $1.5 < \eta < 2.1$ and is capable of measuring photons that have energies greater than 200 MeV. The Zero-Degree Calorimeter (ZDC) is used to measure projectile spectators and, thus, provides us with an indication of collision centrality for each event. The WA80 setup and its individual detectors have been described in detail elsewhere.[12-15]

## 3. TRANSVERSE ENERGY DISTRIBUTIONS

Transverse energy distributions obtained from interactions of 200-GeV/nucleon $^{16}O$ and $^{32}S$ projectiles with various target nuclei are shown in Fig. 2. The data have been described in Refs. 1-3. As was stressed, it is primarily the geometry of the nuclear collision that determines the shape of these distributions. The rise at low values of the transverse energy is due to the relatively large cross section associated with large impact parameters. The bump observed at high $E_T$ values in the case of the heaviest targets results from the fact that collisions with a relatively broad range of central impact parameters involve a nearly constant number of participants. A trigger cut is responsible for the apparent dip at the lowest $E_T$ values while at the high end of the distribution the Gaussian tail is due to fluctuations in the violence of nearly head-on collisions. The two main trends observed are the increase in the transverse energy produced with increasing mass of the colliding system and the increase of transverse energy with increasing bombarding energy. The measured $E_T$ is, as expected, anticorrelated with the energy measured in the ZDC.

It has been shown[1,2] that for oxygen-induced reactions at a given bombarding energy, the transverse energy produced depends on the number of participating nucleons and that the transverse energy/participant is nearly independent of target mass and of collision centrality. In a simple geometrical picture the doubling of the mass of the projectile should increase the number of participants approximately by a factor of $2^{2/3}$, and consequently, an increase in $E_T$ of about a factor of 1.59 was anticipated for the $^{32}S$ + Au reaction relative to the $^{16}O$ + Au reaction. In Fig. 3 the transverse energy spectra from the above two reactions are compared. The $^{16}O$ $E_T$ values have been multiplied by 1.6, which results in an alignment of the tails of the two distributions and indicates that the relationship between the number of

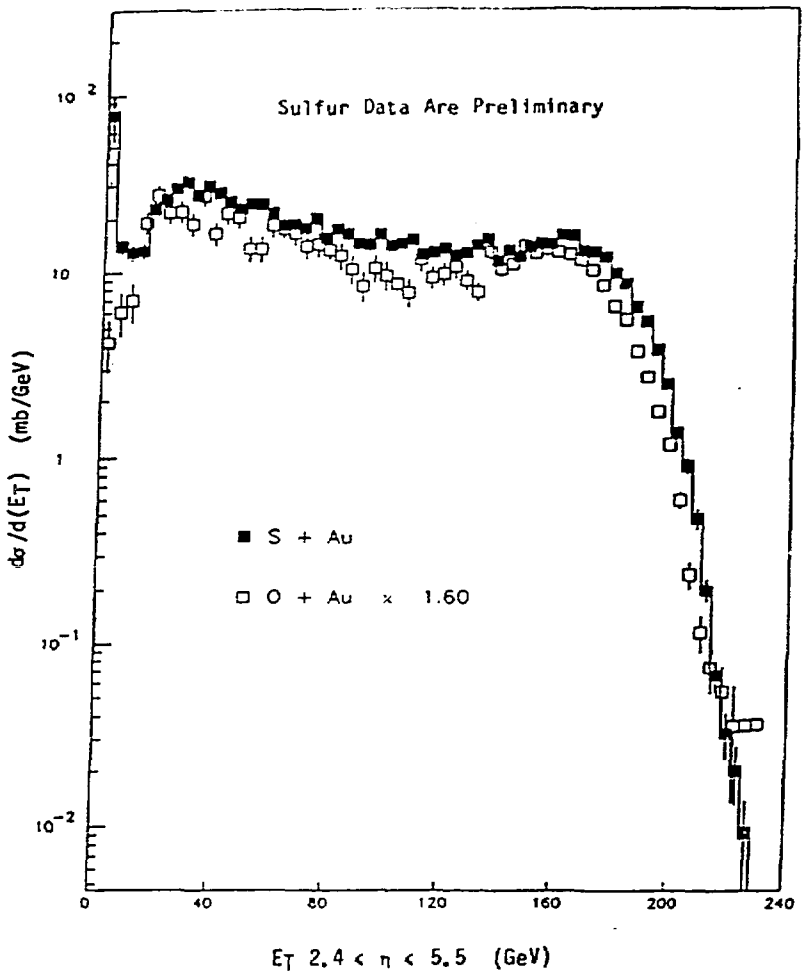


**Fig. 3.** Comparison of transverse energy distributions from $^{16}$O- and $^{32}$S-induced reactions of Au at E/A = 200 GeV. The energy scale of the $^{16}$O + Au data has been multiplied by 1.6 (see text). The sulfur data are preliminary.

participants and the produced transverse energy also holds in the case of sulfur-induced reactions. This point is confirmed in Fig. 4 where $E_T$/participant values are plotted as a function of the energy measured by the ZDC for both oxygen- and sulfur-induced reactions at 200 GeV/nucleon. A nearly constant $E_T$/participant value of 2 GeV is obtained in all cases. The relationship between the number of

participating baryons and the observed ZDC energy was obtained[1-2] via the Mor te Carlo simulation code FRITIOF.[16]

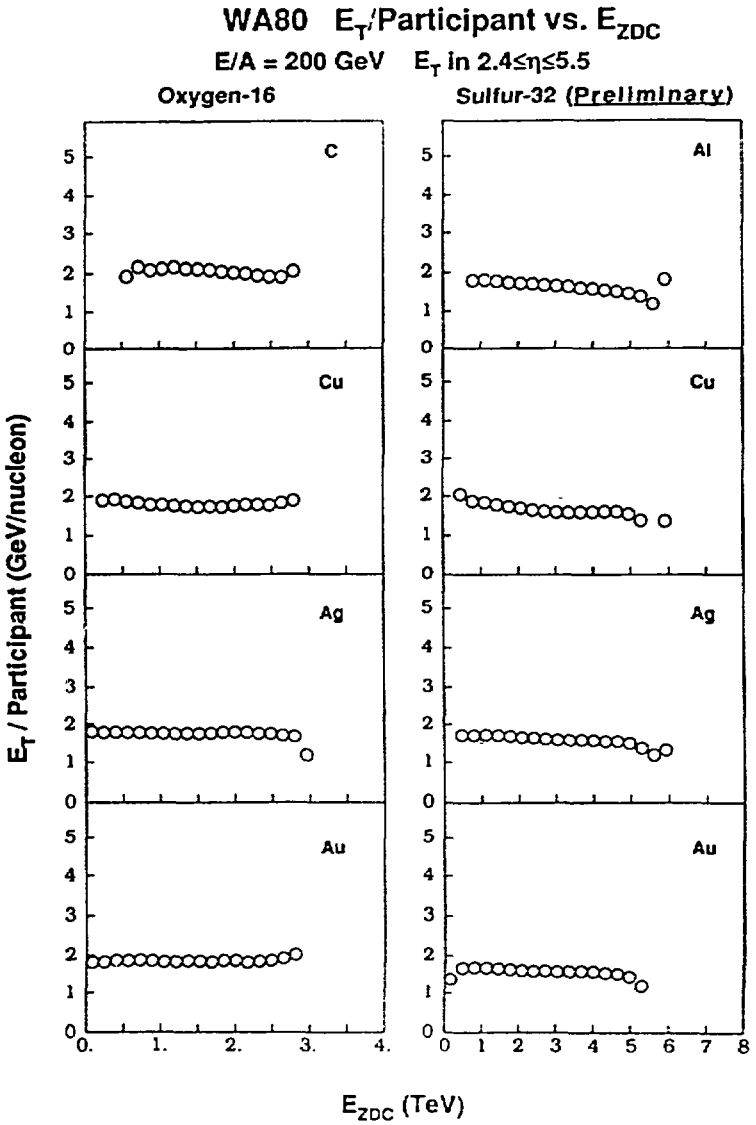


**Fig. 4.** Transverse energy per participant as a function of the energy, $E_{ZDC}$, measured by the Zero-Degree Calorimeter for several target–projectile combinations.

## 4. GLOBAL AND LOCAL FLUCTUATIONS IN MULTIPLICITY AND TRANSVERSE ENERGY

In this study[6] we start with the observation that, in central collisions, $E_T$ and $n_{ch}$ distributions have Gaussian shapes.[7-9] This is illustrated for different ranges of

ZDC energy in Fig. 5 for $^{16}$O + Au at 200 A GeV. It can be seen that the average values and the widths of the distributions are insensitive to collision centrality in the limited range of $E_{ZDC} \lesssim 500$ GeV. The curves in the figure indicate Gaussian fits. The local pseudorapidity interval is $2.5 < \eta < 3.5$, which is symmetric about the nucleon–nucleon center of mass.

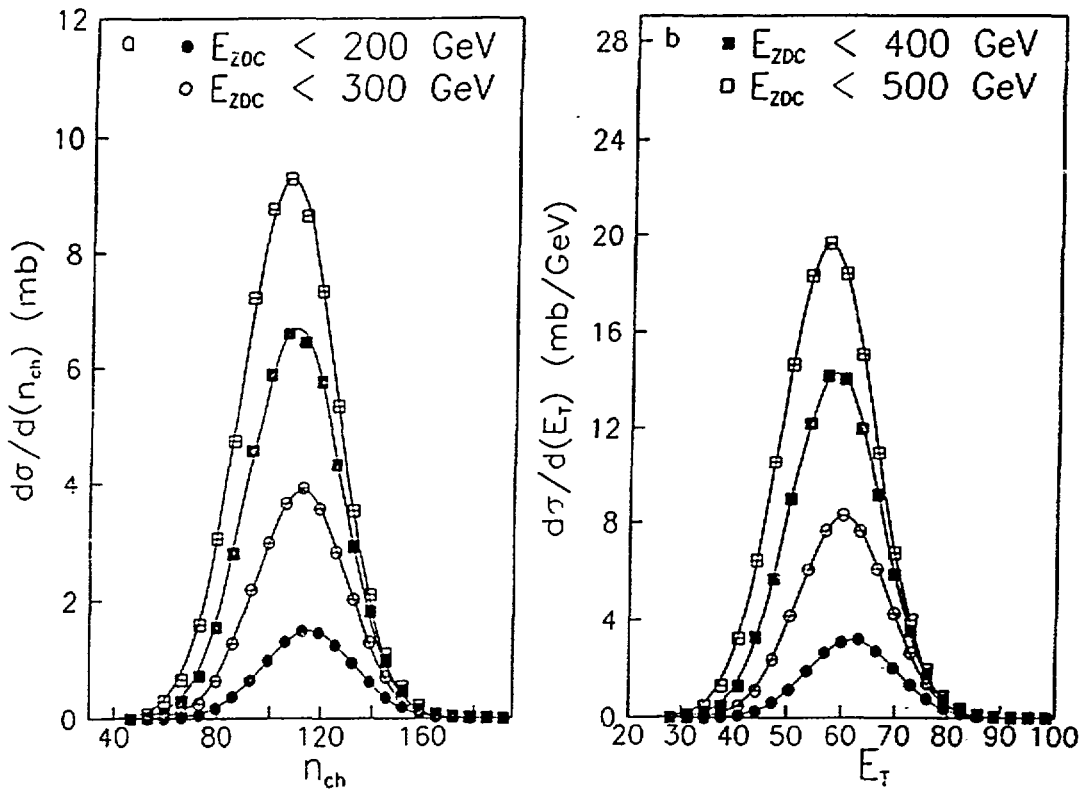


**Fig. 5.** (a) $n_{ch}$ and (b) $E_T$ distributions for central $^{16}$O + Au interactions at 200 A GeV. The curves are Gaussian fits to the distributions from the different ZDC-selected events as indicated in the top of the figures.

The importance of the role of the $\eta$-range can be investigated in terms of the normalized variance of a distribution in $X$ given by $\Omega(X) = V(X)/\langle X\rangle^2$, where $X$ can be either $E_T$ or $n_{ch}$ and where $V(X)$ is the variance of the distribution. From purely statistical considerations, and assuming that a particle produced by a given source has a fixed probability to fall inside the observed region, it can be shown that[6]

$$\Omega(\eta, \Delta\eta) \cdot \frac{1}{\Delta\eta\langle\rho(\eta)\rangle} = const.\,,$$

where $\Delta\eta$ is a region around $\eta$ with $\langle\rho(\eta)\rangle = \frac{dX}{d\eta}$. Sources can be taken to be binary collisions between nucleons from the two reacting nuclei or wounded or participating nucleons.

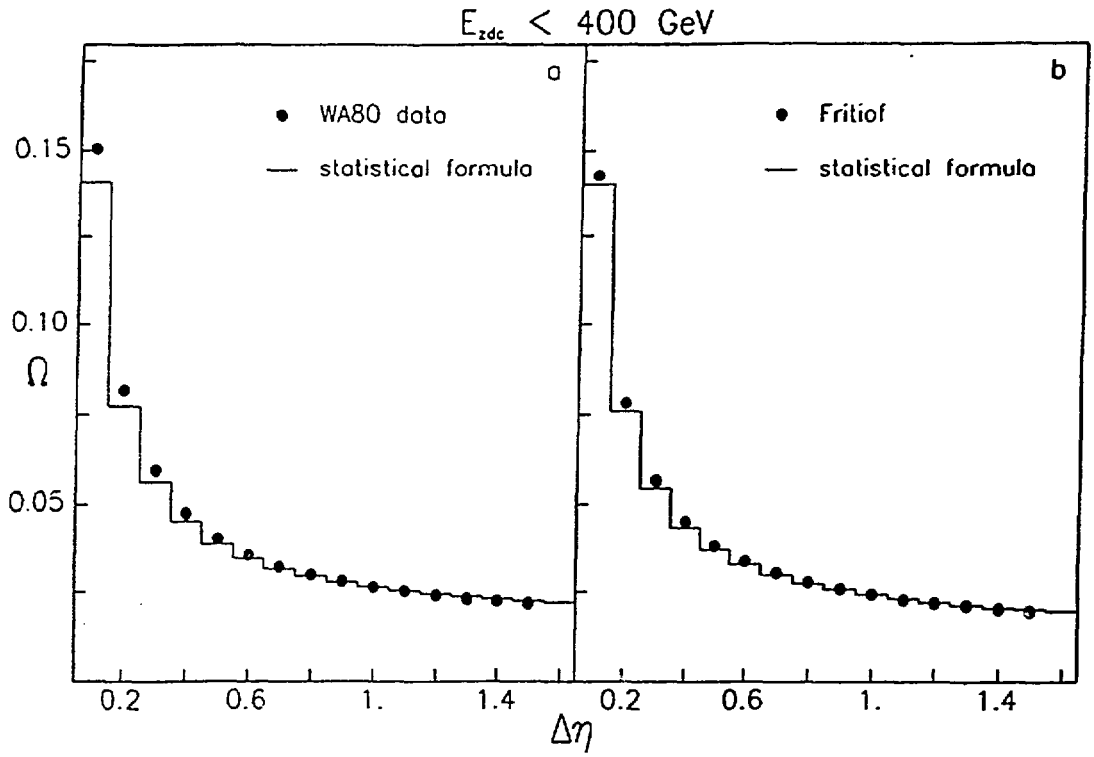


**Fig. 6.** The normalized variance $\Omega$ as a function of $\Delta\eta$ for central $^{16}O$ + Au interactions at 200 A GeV for (a) experimental data and (b) for the FRITIOF sample. The histograms correspond to the calculations from the statistical expresssion given in the text, normalized at $\Delta\eta = 1.0$.

In Figs. 6 and 7, $\Omega$ is shown for $\eta_{ch}$ as a function of $\Delta\eta$ (Fig. 6) and $\eta$ (Fig. 7) both for data and for events calculated by means of the Monte Carlo simulation code FRITIOF,[16] together with the above statistical relationship normalized to data at $\Delta\eta = 1$ in Fig. 6 and at $\eta = 3.05$ in Fig. 7. The ability of the above statistical formula to describe the data indicates that observed fluctuations are, to a large extent, determined by the underlying global fluctuations. Thus, results obtained for a chosen $\eta$-range may be generalized to any other choice of range provided one excludes regions where fluctuations from a different origin may be present, such as fragmentation regions. Furthermore, the results shown in Figs. 6 and 7 indicate that FRITIOF-simulated events exhibit a similar behavior and similar

trends to measured events. Since FRITIOF-calculated ZDC spectra also agree with experimental ZDC spectra, trigger conditions can also be simulated. Consequently, FRITIOF calculations can be used to examine in detail various contributions to the total variance of a given distribution in an effort to establish the origin of observed fluctuations.

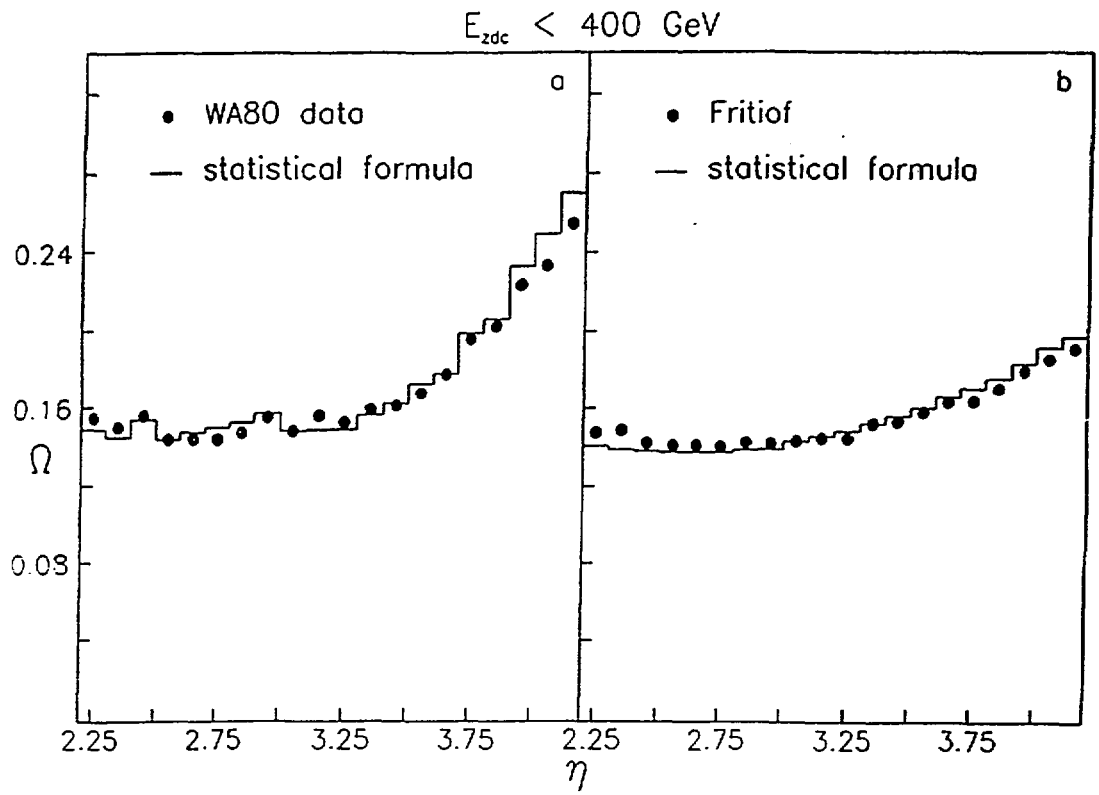


**Fig. 7.** The normalized variance $\Omega$ as a function of $\eta$ for central $^{16}O$ + Au interactions at 200 A GeV for (a) experimental data and (b) for the FRITIOF sample. The histograms correspond to the calculations from the statistical expresssion given in the text, normalized at $\eta = 3.05$.

This approach has been implemented with reference to a formula for the total variance, given by Baym et al.,[9] which is shown to be the sum of four terms, each with a physical meaning in a picture where total fluctuations in nucleus-nucleus interactions consist of a sum of contributions of fluctuations from many independent sources created in early interaction stages. The four contributions to the total variance corresponding to the four terms of the formula of Ref. 9 are:

(1) fluctuations in each of the sources;

(2) fluctuations in the number of sources;

(3) fluctuations emerging from differences in the sources, e.g., due to energy degradations; and

(4) fluctuations arising from damping due to an anticorrelation between above contributions 2 and 3.

The evaluation of the four contributions to the total variance by means of FRITIOF-simulated events leads to several interesting conclusions.[6] Thus, for example, the same trends are observed regardless of whether the sources are taken to be binary collisions between nuclei or the number of participating nucleons. Furthermore, the third contribution listed above (fluctuations emerging from differences in the sources) is consistently small compared to the other terms. This is believed to be a consequence of the long formation time in the FRITIOF model, which makes effects of energy degradation small. The role of the first contribution listed above (fluctuations in each of the sources) is of particular interest and can be elucidated by comparing calculations involving global distributions with those for a limited region of observation ($2.5 < \eta < 3.5$). In the limited $\eta$-region, contribution (1) is important, while it is drastically reduced in the global distribution calculations. This effect is anticipated based on the statistical expression for $\Omega$ given above. Other contributions to the total variance are the same for the global and for the limited-$\eta$-range cases. It is concluded that the apparent importance of the fluctuations from each of the sources in the case when a limited region of phase space is considered is a consequence of the stochastic nature of the sources, where a random process determines if a given particle will fall inside the given region or not.

In the case of global distributions, results indicate that the most important contribution to the total variance is number (2) listed above (fluctuation in the number of sources), while contribution number (4) is also significant. Thus, it is concluded that the observed shapes of the distributions are governed by the distribution of sources, i.e., by the number of participating nucleons or by the number of binary collisions, with some influence of damping effects. The conclusions given here do not depend on whether or not intermittency plays an important role. The very small scales usually associated with studies of intermittent behavior are not within the scope of this analysis.

We return now to the Gaussian nature of the experimental $n_{ch}$ and $E_T$ distributions. The data are plotted as a function of $(X - \langle X \rangle)^2/\langle X \rangle^2$ for central $^{16}O + Au$ *interactions with* $E_{ZDC} < 400$ GeV, *corresponding to about 10% of the* minimum-bias sample in Fig. 8a. In this representation a Gaussian distribution is a straight line, with the two distribution halves superimposed. The slopes are given by $[-2 \cdot \Omega(X)]^{-1}$. In Fig. 8b the corresponding results from the FRITIOF model are shown, and in Fig. 8c the distributions of participants and of binary collisons are indicated. The degree to which the tails of the various distributions are represented by Gaussians is immediately apparent in Fig. 8. Since, as will

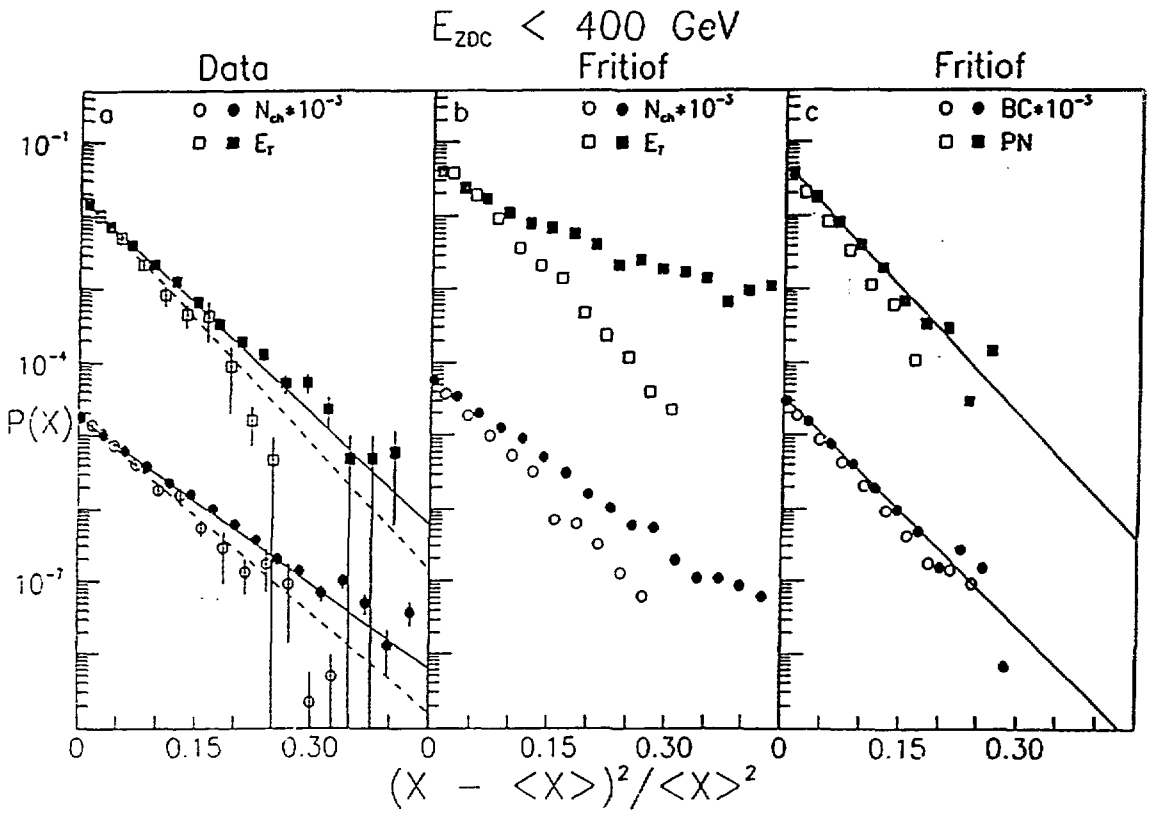


**Fig. 8.** Gaussian representations of (a) experimental $n_{ch}$ and $E_T$ distributions, (b) $n_{ch}$ and $E_T$ distributions from the FRITIOF sample and (c) the source distributions of participants (PN) and of binary collisions (BC). The best-line fits to the points are indicated in (a) for the region $(X - \langle X \rangle)^2/\langle X \rangle^2 < 0.4$ (lower half of the Gaussian is indicated by the dashed line, and the upper half of the Gaussian is shown by the solid line) and in (c) for the region $(X - \langle X \rangle)^2/\langle X \rangle^2 < 0.16$ (upper half of Gaussian only). Filled symbols indicate upper halves of the Gaussians, whereas the open symbols represent lower halves.

be seen in the next section, there is a direct relationship between $E_T$ and energy density ($\epsilon$) distributions, the near-Gaussian tail of the $E_T$ distribution of Fig. 8 implies that the $\epsilon$ distribution will also be nearly Gaussian up to highest values of $\epsilon$. This implies that it is unlikely that there are events present in the central-event data sample with anomalously high values of $\epsilon$.

## 5. ENERGY DENSITIES

As was pointed out in the introduction, reasonable estimates of energy densities attained in nucleus-nucleus collisions may be obtained based on the measured $E_T$ since transverse energy, presumably, directly reflects the amount of thermalized energy. The major source of uncertainty is associated with the estimate of the volume in which the observed energy was contained. The most commonly used method to estimate the energy density is the following relationship first suggested by Bjorken,[4]

$$\epsilon = \frac{1}{\mathcal{A}\tau}\frac{dE_T}{d\eta}\bigg|_{\eta_{max}} , \tag{1}$$

in which the differential transverse energy $\frac{dE_T}{d\eta}\Big|_{\eta_{max}}$ observed at midrapidity is associated with a differential volume of transverse area $\mathcal{A}$ corresponding to the area of nuclear overlap and thickness $\tau$ related to the particle formation time. This estimate has the feature of being a Lorentz invariant valid for the local c.m. frame regardless of whether or not the nuclei are stopped completely. The main disadvantage is that the presently unknown formation time is simply assumed to be 1 fm/c. Furthermore, the Bjorken method should be applied to $dE_T/d\eta$ distributions which exhibit a plateau at midrapidity. Such a situation is expected in the extreme relativistic case, but is not observed at CERN energies. We show estimates of Bjorken energy densities obtained from our data in Fig. 9.

An alternative method is motivated by the observation that, for central collisions, the total transverse energy observed accounts for a large fraction of the energy available in the center of mass, and therefore indicates a large degree of nuclear stopping. In this case an integral estimate of the energy density may be made as

$$\epsilon = \frac{1}{AL}\int d\eta \frac{1}{\sin\theta_{cm}}\frac{dE_T}{d\eta} , \tag{2}$$

where the total available energy has been obtained by integrating the observed $\frac{dE_T}{d\eta}$ distribution. While our $E_T$ measurements are made only in the forward $\eta$ region, the data indicate that it is reasonable to assume a gaussian shape of the $dE_T/d\eta$ distribution for the purpose of integration. The total volume in the center of mass is given by the transverse area $A$ times $L$, the total Lorentz-contracted length of the stopped system, as seen in the center-of-mass frame. Some estimates have assumed

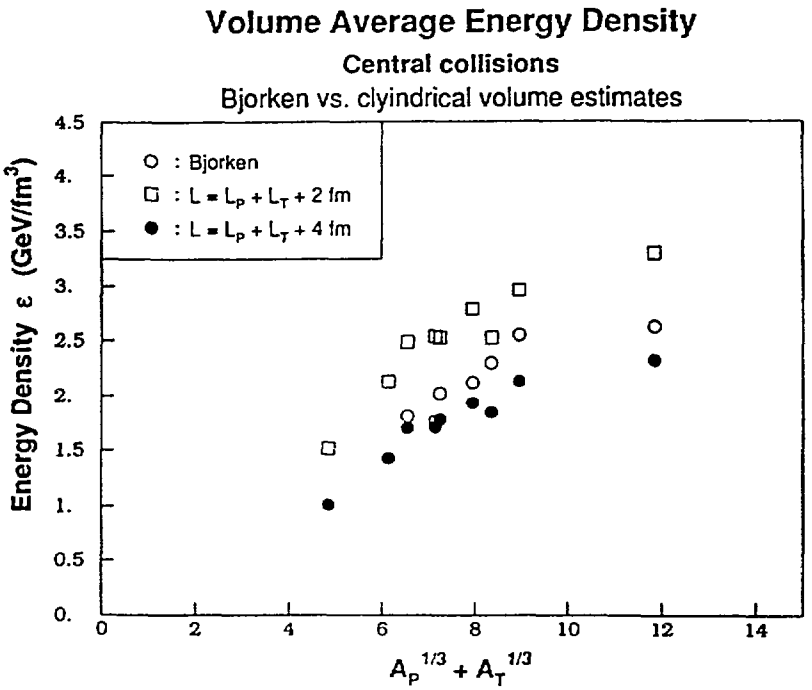


**Fig. 9.** Energy density estimates for 200-GeV/nucleon $^{16}$O- and $^{32}$S-induced reactions as a function of the total thickness of the interacting system. The Pb + Pb points are based on an extrapolation of the observed $E_T$ scaling. See the text for a description of the methods used to make the estimates.

that the initial conditions are such that the smaller projectile is stopped within the target volume[17,18] as suggested many years ago by Landau,[19] and have assumed $L$ to be the contracted target length. It has been shown,[5] however, that these estimates lead to unrealistically high energy density values and that the energy density decreases with increasing thickness of the system, contrary to expectation based on the observation that the stopped energy fraction is nearly constant but less than one. As an alternative to Landau stopping, one may combine the integral

total available energy approach with initial conditions as suggested by Bjorken[4] in which, as in the capacitor-plate analogy, after passing through one another, the receding nuclei are nearly stopped due to the energy stored in the intervening color fields. In this case the appropriate total length can be taken as the sum of projectile and target lengths plus the intervening stopping distance $L_S$. The dependence of this energy density estimate on the total nucleon thickness $A_P^{\frac{1}{3}} + A_T^{\frac{1}{3}}$ is shown in Fig. 9 for $L_S$ values of 2 fm and 4 fm. A stopping distance of $L_S = 4$ fm gives values consistent with those obtained for a 1 fm/c formation time at about 2-3 GeV/fm$^3$ for the heavy systems. This is similar to recent calculations.[20] It can be seen in Fig. 9 that both the integral and differential estimates assuming Bjorken-type initial conditions show a systematic increase with increasing thickness of the system, as might be expected for overlapping color strings, and that the average energy density obtained by these methods is not expected to increase significantly for reactions of Pb + Pb. As is shown below, however, the core energy density is expected to increase substantially with increasing projectile mass.

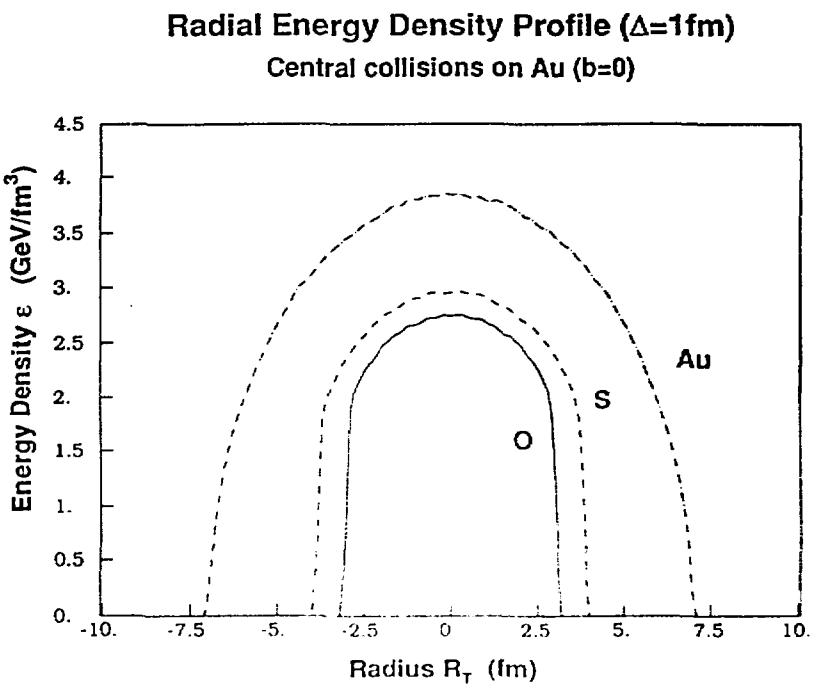


**Fig. 10.** The estimated energy density profile for zero impact parameter collsions of O, S, and Au on Au at 200 GeV/nucleon based on Eq. 1 and the observed scaling of the transverse energy.

In addition to the observation discussed in Section 3, that the total $E_T$/participant is constant when integrated over the forward pseudorapidity region $2.4 < \eta < 5.5$, it is similarly found that $\frac{dE_T}{d\eta}\Big|_{\eta_{max}}$/participant is also constant with a value of about 1 GeV/participant for all systems and impact parameters. Using this information we may generalize Eq. 1 and calculate the radial energy density profile according to the participant nucleon profile. The result is shown in Fig. 10 for zero impact parameter collisions of O, S, and Au on Au at 200 GeV/nucleon. The comparison between the different systems is now much more dramatic than the volume-average comparison of Fig. 9, in that one expects a 30% higher central energy density for Au projectiles. In fact, it is seen that if the energy density necessary for the phase transition corresponds to 3 GeV/fm$^3$, then central collisions of Au nuclei would result in a cylindrical volume having a diameter of about 10 fm with an energy density significantly above the critical value, while other systems would not produce energy densities in the critical range.

## 6. TRANSVERSE MOMENTUM DISTRIBUTIONS OF NEUTRAL PIONS

The primary purpose of the single-arm photon spectrometer SAPHIR is to measure the spectra of direct photons which may be emitted from the QGP. Photons and other electromagnetic probes, because of their noninteracting nature, are believed to be the best tools with which early reaction stages can be explored. The direct photon spectra can be extracted from the data only after the very large number of photons produced by decaying neutral pions and $\eta$ mesons have been accounted for. This procedure is very complicated, and the final result is very sensitive to a number of factors such as acceptance, shower identification, and neutral pion reconstruction. The direct photon spectra that we have obtained to date[3,11] are too preliminary to be included here, and are in the process of being reevaluated.

Somewhat less sensitive to the factors mentioned above are the spectra of neutral pions which are obtained by invariant mass reconstruction. Results have been presented in Ref. 10. Neutral pion distributions obtained from the $^{16}$O + Au reaction at 200 GeV/nucleon are shown in Fig. 11 as a function of transverse momentum, $p_T$, for two different ranges of collision centrality. Exponential fits in the transverse momentum range $0.8 < p_T < 2$ GeV/c are also shown. The slope parameters, $T$, are 189 $\pm$ 5 MeV/c for peripheral and 220 $\pm$ 5 MeV/c for central

collisions, respectively. The slopes are extrapolated to higher and lower $p_T$ regions. The following three main features of the data are to be noted: (1) Over most of the $p_T$ range, the value of the slope parameter is significantly higher for central collisions than for peripheral collisions; (2) in the low $p_T$ region lower values of the slope parameter are observed than in the central $p_T$ region, but only in the case of

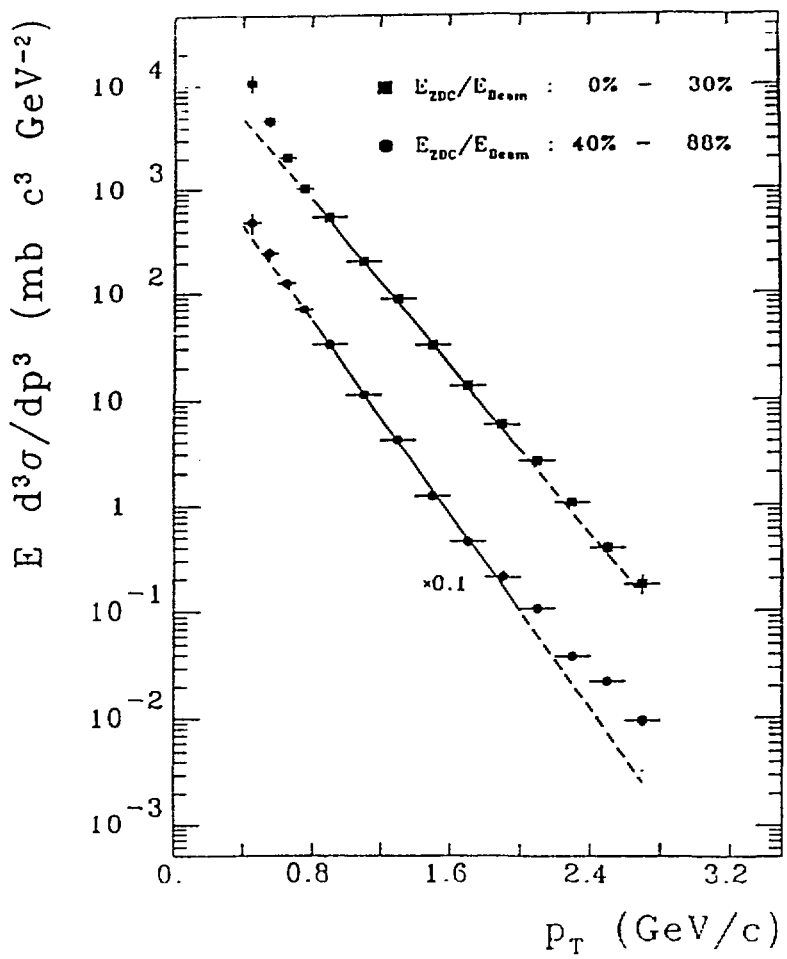


**Fig. 11.** Invariant $\pi^0$ cross sections from collisions of 200-GeV/nucleon $^{16}O$ projectiles with Au target nuclei measured in the pseudorapidity range $1.5 \leq \eta \leq 2.1$ for different ranges of the energy, $E_{ZDC}$, measured in the Zero-Degree Calorimeter. The squares correspond to central collisions and the circles to peripheral collisions. Exponential functions are fitted to the spectra in the range $0.8 \leq p_T \leq 2$ GeV/c and are extrapolated to the full $p_T$ range as indicated by the dashed lines.

central collisions; and (3) at high $p_T$ values, no change is observed in the slope parameter for central collisions, while peripheral collisions exhibit a clear deviation from central $p_T$ slope parameters to much higher values. This last behavior is similar to that observed in the data of $p + p$ collisions at similar energies. It is attributed to the onset of hard QCD scattering, which is, presumably, obscured by nuclear effects in central collisions. At lower values of $p_T$ the changing of the slope parameter with centrality can be understood on the basis of a hydrodynamic model with isotropic expansion of a fireball.[21] The increased cross section at low $p_T$ values in central collisions (see above and Fig. 11) is described in a thermodynamical picture as being a consequence of the rescattering of secondary pions.[22]

## 7. SUMMARY

The following main points have been made:

1. The broad features of measured transverse energy distributions are determined by the collision geometry.
2. The transverse energy per participating baryon produced in the pseudorapidity range from 2.4 to 5.5 has a value of about 2 GeV and does not vary significantly with projectile mass, target mass, or collision centrality.
3. $E_T$ and $n_{ch}$ distributions are determined primarily by source distributions.
4. Either the number of participants or the number of binary collisions can be used to characterize $E_T$ and $n_{ch}$ distributions.
5. When limited $\eta$ regions are considered, the stochastic nature of the sources will broaden the observed $E_T$ and $n_{ch}$ distributions. Observed local distributions are determined by global ones.
6. Volume-averaged energy densities increase with increasing projectile energy but not significantly with increasing projectile size.
7. Energy densities attained in the central core do increase with projectile size.
8. Slope parameters of neutral pion transverse momentum spectra have higher values for central than for peripheral events.
9. Peripheral-collision neutral pion spectra display a marked change of slope at high values of transverse momenta in contrast to central-collision spectra.

## REFERENCES


a. Oak Ridge National Laboratory,† Oak Ridge, Tennessee 37831.
b. Gesellschaft für Schwerionenforschung (GSI), D-6100 Darmstadt, West Germany.
c. University of Münster, D-4400 Münster, West Germany.
d. University of Lund, S-22362 Lund, Sweden.
e. Lawrence Berkeley Laboratory, Berkeley, California 94720.
f. University of Tennessee, Knoxville, Tennessee 37996.
* On leave of absence from the Institute of Nuclear Studies, Warsaw, Poland.
† Operated by Martin Marietta Energy Systems, Inc., under contract DE-AC05-84OR21400 with the U.S. Department of Energy.

1. R. Albrecht *et al.*, Phys. Lett. B **199**, 297 (Dec. 1987).
2. S. P. Sorensen *et al.*, Proceedings, 6tl. International Conference on Ultrarelativistic Nucleus-Nucleus Collisions, Schloss Nordkirchen, West Germany, August 24-28, 1987, Z. Phys. C **38**, 3 (Apr. 1988).
3. G. R. Young *et al.*, Proceedings, Seventh International Conference on Ultrarelativistic Nucleus-Nucleus Collisions, Lenox, Massachusetts, September 26-30, 1988; to be published in Nuclear Physics A.
4. J. D. Bjorken, Phys. Rev. D **27**, 140 (1983).
5. T. C. Awes for the WA80 Collaboration, Proceedings, XXIV Recontres de Moriond, Les Arcs, Savoie, France, March 13-19, 1989; to be published.
6. R. Albrecht *et al.*, Lund University Preprint LUIP-8903 (May 1989).
7. I. Otterlund *et al.*, Proc. Int. Conf. on Physics and Astrophysics of Quark-Gluon Plasma, Bombay, India, Feb. 1988; Lund University Preprint LUIP-8806 (1988).
8. F. Corriveau *et al.*, Z. Phys. C **38**, 15 (1988).
9. B. Baym, G. Friedman, and I. Sarcevic, Phys. Lett. B **219**, 205 (1989).
10. R. Albrecht *et al.*, Phys. Lett. B **201**, 390 (Feb. 1988).
11. R. Santo *et al.*, Proceedings, Seventh International Conference on Ultrarelativistic Nucleus-Nucleus Collisions, Lenox, Massachusetts, September 26-30, 1988; to be published in Nuclear Physics A.
12. R. Albrecht *et al.*, "Study of Relativistic Nucleus-Nucleus Collisions at the CERN SPS," CERN Report CERN/SPSC/85-39 (August 1985).
13. H. H. Gutbrod *et al.*, pp. 42-52 in Proceedings, International Workshop on Gross Properties of Nuclei and Nuclear Excitations XV, Hirschegg, Austria, January 12-17, 1987, GSI and Institut für Kernphysik, Darmstadt, F.R.G., 1987.
14. T. C. Awes *et al.*, Nucl. Instrum. Methods Phys. Res. **A279**, 479 (1989).
15. G. R. Young *et al.*, Nucl. Instrum. Methods Phys. Res. **A279**, 503 (1989).
16. B. Andersson, G. Gustafsson, and B. Nilsson-Almqvist, Nucl. Phys. **B281**, 289 (1987); B. Nilsson-Almqvist and E. Stenlund, Comput. Phys. Commun. **43**, 387 (1987).
17. A. Bamberger *et al.*, Phys. Lett. B **184**, 271 (1987).
18. J. Stachel and P. Braun-Munzinger, Phys. Lett. B **216**, 1 (1989).
19. L. D. Landau, No. 88, Izv. Akad. Naul. SSSR, Ser. Fiz. **17**, 51 (1953).
20. K. Werner *et al.*, Phys. Lett. B **219**, 111 (1989).
21. K. S. Lee and U. Heinz, Theoretische Physik Regensburg TPR-88-16, to be published in Zeitschrift für Physik.
22. E. V. Shuryak, Novosibirsk, preprint 87-142; E. V. Shuryak, Phys. Lett. B **207**, 345 (1988).